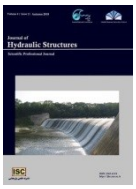
Journal of Hydraulic Structures
J. Hydraul. Struct., 2020; 6(3):1-20
DOI: 10.22055/jhs.2020.34556.1145

OPEN ACCESS



Application of a New Approach in Optimizing the Operation of the Multi-Objective Reservoir

Alireza Donyaii [1]
Amirpouya Sarraf [2]
Hassan Ahmadi [1]

Abstract

The application of optimization tools and techniques to operate the reservoir on a Multi-objective basis under the circumstances of climate change is unavoidable. The present study utilizes the Multi-Objective Farmland Fertility Optimization (MOFFA) algorithm to derive optimum rules on the operation of the Golestan Dam in Golestan province under circumstances of climate change. The two targets of reducing vulnerability as well as maximizing reliability under baseline conditions (from April 2006 to October 2018) and climate change conditions (from April 2021 to October 2033) have been formulated for such guidelines. Results revealed that under climate change circumstances, the river flow decreased by 0.17 percent of the baseline period, although the temperature was increased by 20% as well as the rainfall decreased by 21.1%. However, the extent of vulnerability variations in baseline and climate change was 16-45% and 10-43%, respectively. The range of reliability variations in baseline and climate change circumstances was 47-90% and 27-93%. The vulnerability has also been measured at 29 percent and 27 percent for baseline and climate change, respectively, with 75 percent reliability. The increase in release rates for climate change in comparison with baseline circumstances and higher modification of release rates from the reservoir to demand and stronger dam efficiency in changing circumstances showed the comparison of releases and the water shortage requirements for each of Pareto points.

Keywords: Climate Change, Decision Making Rules, Farmland Fertility Optimization Algorithm, Reliability, Vulnerability.

Received: 05 August 2020; Accepted: 01 September 2020

[1] Department of Civil Engineering, Roudehen Branch, Islamic Azad University, Roudehen, Iran
[2] Department of Civil Engineering, Roudehen Branch, Islamic Azad University, Roudehen, Iran. sarraf@riau.ac.ir **(Corresponding Author).**

CC BY

1. Introduction

Operation and performance management of dam reservoirs plays an important role in the management of water resources in each region. Due to the limited water resources, the operation of dam reservoirs is of special importance because of its economic value resulted from the optimal operation of water resources, increasing water demands, and shortage of available water resources. Therefore, it is essential to use a method that provides optimal operation management of dam reservoirs, especially in climate change circumstances. Hence, decision-making options must be extracted using all objectives and multi-objective optimization models. Thus, in the last two decades, a group of approximate solution algorithms called meta-heuristic algorithms in optimal operation of the reservoir system has been developed that effectively and efficiently explore the search space and prevent the solution method from being trapped within the confines of the search space [1]. In recent decades, using of artificial intelligence models has been widely applied in all aspects of science and technology from air pollution predictions [2] to water resources management [3, 4]. Many of these methods have been used for multi-objective optimization of water resources systems, especially dam reservoirs. One of their most important and widely used are multi-objective evolutionary algorithms, which in each iteration provide a set of optimal solutions that can be presented in the form of the Pareto curve.

Ashrafi [5] used the multi-objective particle swarm optimization algorithm to investigate the different management policies of multi-reservoir systems and their impact on the demand supply and hydropower generation in the Great Karun River basin. The results showed that the effects of different system reservoirs on energy production and demand supply are not the same across the basin and they should be considered carefully for achieving maximum efficiency of the multi-reservoir system in meeting different demands and for extracting the optimal operating rule curves. Ashrafi et al. [6] presented and applied a Self-adaptive version of Melody Search algorithm to obtain operating rule curves for multi-reservoir systems. After evaluating the capability of Melody search algorithm with eight benchmark problems and comparing it with other well-known metaheuristic algorithms, they used the Melody search algorithm for optimal operation of a four-reservoir system located in Karkheh river basin to meet agricultural requirements. Wu et al. [7] conducted a multi-objective operation of hydropower reservoirs using NSGA-II and objective functions to maximize profits of water supply and hydropower generation and minimize the water shortage for environmental demandsand proved the efficiency and effectiveness of the proposed algorithm and model by using it in the Lango reservoir on the Yellow River of China.

The problem of a reservoir operation optimization was studied by Sayyafzadeh et al. [8] using the Artificial Bee Colony algorithm (ABC) and the results were compared with Genetic Algorithm (GA). With the Particle Swarm Optimization (PSO), ABC and GA, Hossain & EI-Shafie [9] solved the operational optimization of the reservoir. The results indicated that the ABC algorithm was best adapted for water demand supply and water shortage management.

Ashofteh et al. [10] used the multi-purpose genetic program to optimize the Aydoghmush dam reservoir in East Azerbaijan province in Iran under baseline and climate changeconditions. The optimization results revealed that the rules of reservoir performance that are involved in climate change lead to an improvement from 29% to 32% in reservoir performance due to climate change compared to baseline. Ehteram et al. [11] applied the kidney algorithm, to generate an optimal operation of the Aydoghmoush reservoir in eastern Azerbaijan province in Iran to decrease irrigation deficit downstream of the dam. They compared the results of the kidney algorithm with other evolutionary algorithms, including bat (BA), genetic (GA), particle

swarm (PSO), shark (SA), and weed algorithms (WA). The results showed that the kidney algorithm provided the best performance against the other evolutionary algorithms.

Donyaii et al [12] after introducing the whale multi-objective optimization algorithm, they evaluated its performance as optimal operation of the Boostan dam reservoir based on the Conflict Resolution Method of Kalai & Smorodinsky. The optimization results showed better performance of the whale multi-objective algorithm than NSGA-II, in both objective functions, as well as the operation policies of Boostan Dam Reservoir have a very good agreement with the whale multi-objective algorithm as the result of Kalai & Smorodinsky method of Conflict resolution. Afkhamifar & Sarraf [13] evaluated the performance of two models of Extreme Learning Machines (ELM), Artificial Neural Network (ANN) and the combination of two models with wavelet transmission algorithms (W-ELM and W-ANN). They revealed the hybrid model of W-ELM-QPSO has a better performance than other models and also in addition to predicting power, this model has a high speed in terms of training and testing speed than other models.

In the present study, the development and application of multi-objective Farmland fertility optimization algorithm (MOFFA)was proposed as a multi-objective optimization tool, which has not been addressed in previous researches and is considered as an innovation in the field of water resources. Moreover, the optimal operation rules of the single-reservoir system of Golestan Dam (Golestan province) in Iran in baseline conditions (from April 2006 to October 2018) and climate change circumstances (April 2021 to October 2033) using MOFFA algorithm, with two objectives of minimizing vulnerability and maximization reliability index in demand-supply were determined and compared in the mentioned periods.

The methods applied in this research are as follows:

- Assessing climate change parameters;
- Simulation of rainfall-runoff processes for determining Golestan Dam reservoir discharge volume in Iran;
- Estimation of baseline water demand volume and climate change conditions; multi-objective operating rules extraction (based on three variables of storage volume, demand volume and discharge to the reservoir) in climate change and baseline circumstances;

Ultimately, the procedures for this investigation were to compare optimum allocation policies in baseline and climate change with the performance measures and efficiency indices of the reservoir.

2.Optimization model development

The simulation of the reservoir through the continuity equation would be described as follows:

$$S_{(t+1)} = S_{(t)} + Q_{(t)} - Re_{(t)} - Sp_{(t)} - Loss_{(t)} \quad (1)$$

$$Loss_{(t)} = A_{(t)} \times Ev_{(t)} \quad (2)$$

$$A_{(t)} = aS_{(t)}^3 + bS_{(t)}^2 + cS_{(t)} + d \quad (3)$$

Where $A_{(t)}$ implies to the reservoir surface in the t-th month, $Ev_{(t)}$ is the net evaporation from the reservoir (the difference among the amount of rainfall and evaporation in *the t-th*

month), and a , b , c , and d imply the constant coefficients of the volume-area equation of the reservoir for the Golestan Dam reservoir. Overflow of the reservoir imposes some constraints on the calculations as follows:

$$S_{P_t}=\begin{cases} S_t + Q_t - Re_t - Loss_{(t)} - S_{max} if S_t + Q_t - Re_t - Loss_{(t)} > S_{max} \\ 0 \qquad\qquad if S_t + Q_t - Re_t \le S_{max} \end{cases} \tag{4}$$

Other constraints are as follows:

$$S_{min} \le S_t \le S_{max} \tag{5}$$

$$Re_{min} \le Re_t \le Re_{max} \tag{6}$$

Where S_{max} and S_{min} imply the maximum and minimum volumes of the reservoir, Re_{max} and Re_{min} are referred to as the maximum and minimum releasable volumes from the reservoir, respectively [14].

Two objective functions have been used in the present study to mitigate vulnerability and optimize the reliability index in baseline and climate change circumstances based on Eqs. (7, 8) [15]:

$$Minimize F_1 = \frac{\sum_{t=1}^{T}(D_t - Re_t | Re_t < D_t)}{[N_{t=1}^{T}(Re_t < D_t)], D_{Max}} \qquad \forall_t = 1.2 \ldots . T \tag{7}$$

$$Maximize F_2 = \frac{N_{t=1}^{T}(D_t - Re_t | Re_t \ge D_t)}{T} \qquad \forall_t = 1.2 \ldots . T \tag{8}$$

Where F_1 implies the objective function of a vulnerability index, F_2 is the objective function of reliability index, D_t is referred to as the demand volume throughout the t-th period, D_{Max} implies the maximum water demand in the operating period, $N_{t=1}^{T}\left(Re_t < D_t\right)$ implies the number of months of water shortage, and $N_{t=1}^{T}\left(D_t - Re_t | Re_t \ge D_t\right)$ implies the number of months of water supply.

$$S_t \ge S_{min} \qquad \forall_t = 1.2 \ldots . T \tag{9}$$

$$Re_t \le Re_{max} \qquad \forall_t = 1.2 \ldots . T \tag{10}$$

In the event of violations of constraints, 9 and 10, penalty functions will be introduced to the objective functions as Eq. (11) Eq. (12) as the following:

$$F_1(or F_2) = F_2(or F_1) \pm \left[A', \left(\frac{S_{min} - S_t}{S_{max} - S_{min}}\right) + B'\right] \qquad \forall_t = 1.2 \ldots . T \tag{11}$$

$$F_1(or F_2) = F_2(or F_1) \pm \left[C', \left(\frac{Re_t}{D_{Max}}\right) + D'\right] \qquad \forall_t = 1.2 \ldots . T \tag{12}$$

Where $\left[A'.\left(\frac{S_{min} - S_t}{S_{max} - S_{min}}\right) + B'\right]$ implies the penalty function achieved from the violation of Eq.

(9), and $\left[C'.\left(\frac{Re_t}{D_{Max}}\right)+D'\right]$ is referred to as the penalty function resulted from the violation of Eq. (10). A' to D' coefficients imply the positive constants of penalty functions with A'=1, B'=0.5, C'=1, and D'=16 values [15].

2.1. Operation rule curve

In the existing study, the rule of decision is derived based on Eqs. (13, 14) for the operation of the Golestan Dam single-reservoir system to minimize the vulnerability resulted from the system shortage and to provide the necessary demand, and also to optimize the demand-supply reliability using a MOFFA algorithm:

$$Re_{\mathrm{bt}} = \mathrm{g}_1(Q_{\mathrm{bt}} + \mathrm{S}_{\mathrm{bt}} + \mathrm{D}_{\mathrm{bt}}) \qquad \forall_t = 1.2\ldots..T \qquad (13)$$

$$Re_{f\mathrm{t}} = \mathrm{g}_2(Q_{f\mathrm{t}} + \mathrm{S}_{f\mathrm{t}} + \mathrm{D}_{f\mathrm{t}}) \qquad \forall_t = 1.2\ldots..T \qquad (14)$$

$\mathrm{g}_1\left(Q_{\mathrm{bt}} + \mathrm{S}_{\mathrm{bt}} + \mathrm{D}_{\mathrm{bt}}\right)$ of the first option implies the rule from MOFFA in the baseline operating period for baseline circumstances, and $\mathrm{g}_2\left(Q_{f\mathrm{t}} + \mathrm{S}_{f\mathrm{t}} + \mathrm{D}_{f\mathrm{t}}\right)$ of the second option implies the rule from MOFFA in the climate change operating period for climate change circumstances. The b index is for baseline circumstances, and f index is for climate change circumstances [10].

3. Case1: Farmland Fertility Algorithm (FFA)

The new farmland fertility optimization algorithm (FFA) introduced by Shayanfar and Soleimanian Gharehchopogh [16] was used to derive rules of the Boostan Dam Reservoir operation. According to the FFA optimization algorithm, the farmers in their land decide the quality of the soil for each farmlands area. The primary reason for variability of soil quality is that special materials are composed and added. Farmers, therefore, use various materials to enhance agricultural land quality.

This means that such materials can boost or reduce the soil quality when applied to soil in agricultural land. The determination of these materials to improve the soil quality is based on the experimental materials of farmers with each type of soil and the results of each improvement in soil quality. The key steps to determine the best soil quality materials can be defined in mathematical terms as follows:

3.1. First stage: initialization

The initialized population production is based on the following criteria at this stage:

- Taking into consideration the number of farmland sections (number of optimization parts indicated by k).
- Taking into account the number of solutions available in each section, (number of current solutions in each agricultural segment which is indicated by n).

This first step in generating the overall population N (Ahmed et al. 2019) is defined as follows in mathematical equation:

$$N=k*n \qquad (15)$$

Where, k is more than zero and an integer number. The constant k is considered for search space partitioning (because farmers split their land into separate sections). The value varies from one to N. In this article, the best solution and its value is defined by trial and error. The FFA algorithm shows very low performance when the value is above eight. Therefore, k can be seen as $2 \leq k \leq 8$. In addition, n is an integer count. The trial and error process in this work are also determined. The solution from every search area is defined. In the first step, the following equation produces a random solution with the upper and lower limits of each U_j and L_j variable, respectively [16]:

$$X_{ij} = L_j + rand(0,1) \times (U_j - L_j) \tag{16}$$

Where the j=[1. . . D] in the optimization problem represents the dimension of the variables x and is based on the overall population number equivalent to [1. . ..N]

Figure 1 Demonstrates that the farmland is divided into three parts, each part has its own local memory and global memory, and Part A has lowest quality soil. Within the next section, each stage is represented in the mathematical expression.

3.2. Second stage: finding of soil quality on every farmland section

The fitness of all current search solutions was assessed in this stage. Furthermore, soil quality can be calculated as follows on each part of a field [16]:

$$\begin{aligned} &Section_s = X(\alpha_j), a = n^*(s-1) : n_* ss = \{1,2,...,k\}, \\ &j = \{1,2,...,4\} \end{aligned} \tag{17}$$

For each section of the agricultural field, the average value of existing solutions is used to assess their quality. The individual segments of the agricultural land have been identified at this point of agricultural fertility. The solutions and their average have also been determined for each segment.

3.3. Third stage: update memories

The local memory and global memory were modified at this point. One of the best solutions for each part of the farmland are stored in the local memory and the best solutions from each part are stored in a global memory. In accordance with Equation (18) and (19), the number of best local memories and the number of best global memory are calculated [16].

$$M_{local} = raund(t*n),\ 0.1 < t < 1 \tag{18}$$

$$M_{Global} = raund(t*n),\ 0.1 < t < 1 \tag{19}$$

In which, the number of solutions stored in global memory is expressed by MGlobal. Mlocal is the amount of the solution stored in local memory. The approaches have been developed based on the appropriateness of the local and global memories. In addition, the two memories are updated at this stage [16].

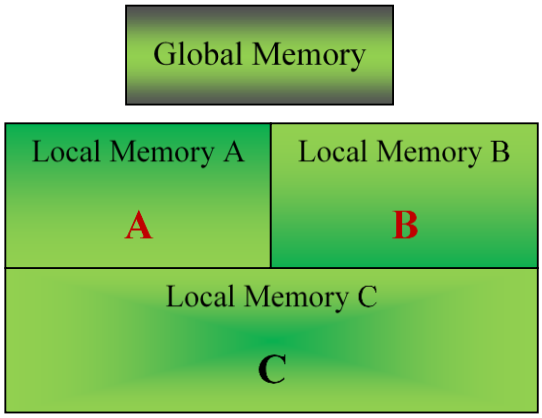


Figure 1. Partitioned Example of Farmland and Local Memory and Global Memory.

3.4. Fourth stage: altering soil quality in each agricultural section

The soil quality was calculated by equation (17) in the third stage of each section. In the corresponding local memory, the best solution in each part of the agricultural land was stored. In addition, the best solution is stored in the global memory for all parts. At this stage, it would be necessary to update the solutions for the worst section and enhance its consistency with more adjustments. The best solution for the global memory can thus combine all existing solutions in the worst part. As in Equation (20) and (21), this can be expressed mathematically [16].

$$h = a * rand(-1,1) \tag{20}$$

$$X_{new} = h*(X_{ij} - X_{M_{Global}}) + X_{ij} \tag{21}$$

Where, the XMGlobal solution is a random one between current global memory solutions and α is a number that should be evaluated at the initiation of farmland fertility between zero and one. Xij is a solution that is chosen to make improvements in the worst part of agricultural land. In addition, h is a decimal number determined by Eq. [20]. The current solution is also *Xnew*. This solution was updated [16].

After the preceding improvement has been made, the following equations (22) and (23) are applied as a combination of the current solutions in each part (except the worst section):

$$h = \beta * rand(0,1) \tag{22}$$

$$X_{new} = h*(X_{ij} - X_{uj}) + X_{ij} \tag{23}$$

Where, among existing search solutions, Xuj is a random solution. This implies that all proposed approaches in sections are randomly selected. β is a number that should be calculated at the beginning of the farmland fertility cycle between zero and one. Xij is the worst solution and was selected to incorporate improvements in the system. h is a decimal number. A new Xnew solution is given after the improvements have been made [16].

3.5. Fifth stage: soil's combination

As we express algorithms in part 1 theoretically, at this stage farmer are deciding to combine every soil in the parts of farmland according to the best local (Best Local) solutions available in the final stage of each section. Consequently, the mixture with the best in local memory is provided. So that not all solutions available in all areas are merged with local memory, and, in this process, some of the solutions at all places are merged with the best solution ever found (Best Global) to increase the quality of solutions in each section of the farmland. The composition of the solution being considered with Best Global and Best Local is calculated by the following Equation:

$$H = \begin{cases} X_{New} = X_{ij} + \omega_1 * \left(X_{ij} - Best_{G;obal}(b)\right) & Q > rand \\ X_{New} = X_{ij} + rand(0,1) * \left(X_{ij} - Best_{local}(b)\right) & else \end{cases} \quad (24)$$

Two specific approaches can be used to build a new solution in Equation 24. Q is a variable between zero and one and has to be modified in the optimization algorithm at fist. The Q parameter defines the degree to which solutions are merged with BestGlobal. ω_1 is an integer number that should be assessed at the beginning of the process and its amount was gradually reduced depending on the repetition of the optimization algorithm (equation 25). Xij is a solution chosen from all parts to incorporate the changes. The implemented changes have therefore led to the development of a new Xnew solution [16].

$$\omega_1 = \omega_1 * R_v, \ 0 < R_v < 1 \quad (25)$$

3.6. Sixth stage: final conditions

The potential solutions currently available in the search area will be evaluated by objective function at this point. No matter how many sections, all available solutions in the search field are implemented at this stage. Therefore, in the search area the degree of fitness is calculated for each of the available solutions. Final conditions should be assessed at the end of agricultural fertility. The algorithm ends when we confirm the last condition. If not, the algorithm will keep on working on determining the final conditions. Figure 2 [16] demonstrates the flowchart of the FFA optimization algorithm.

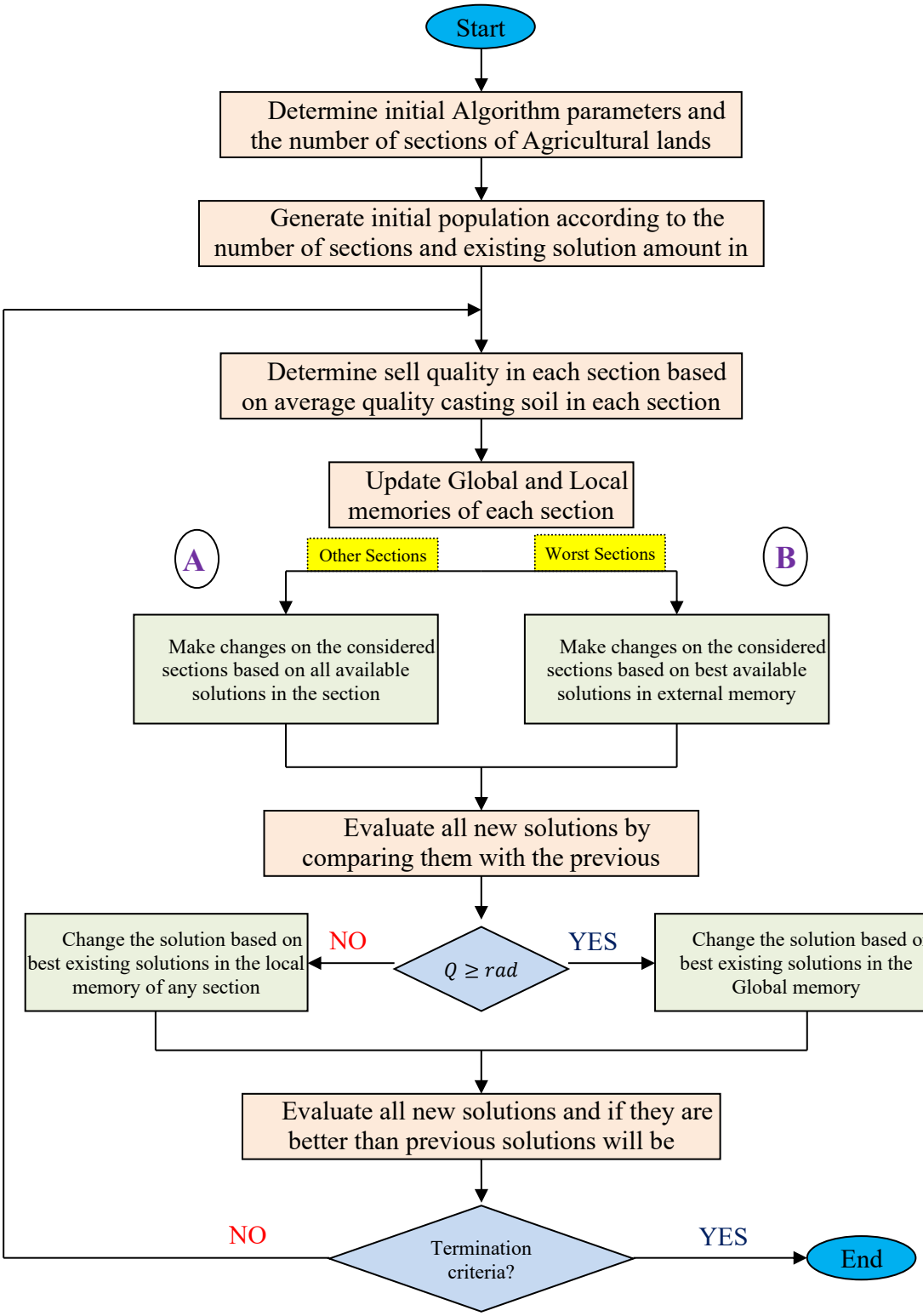


Figure 2. Flowchart of Farmland Fertility Algorithm

4. Results and discussion

4.1. Estimation of climate change parameters

In this study, in order to obtain a more realistic approximation, by averaging three scenarios (i.e., rcp 2.6, rcp 4.5, and rcp 8.5), a new scenario named as the mean scenario was proposed after downscaling the canesm2 climate model with sdsm 4.2 software. The findings show that the monthly average temperature increases by up to 20% in climate change conditions in all scenarios. Analyzing the average monthly precipitation variations have shown that in the climate change condition, the precipitation rate decreases up to 21.1 percent regarding to the baseline (table 1).

Table 1. The Golestan reservoir's SDSM results in predicting rainfall values based on different scenarios

comparison	RCP 2.6	RCP 4.5	RCP 8.5	Mean RCP
Climate change Rainfall values compared to baseline period in percent	-21.9	-22.9	-18.4	-21.1

4.2. Simulation of rainfall-runoff under climate change conditions

A second-order Neuro-Fuzzy model with a Gaussian membership function were conducted to simulate the rainfall-runoff process focusing on the climate change phenomena at the entrance to Golestan Dam, including 20 training epochs and 10000 iterations for 95% of training data (in each prediction). ANFIS's best influence radius for calculating the rainfall-runoff simulation process reached 0.04.

Table 2 shows the statistical indices for different types of ANFIS arrangements at the entrances of Golestan dam reservoir. In this regard, the best ANFIS prediction model was obtained for 95% of the training data with a radius influence of R_e=0.04, 20 training epochs, and 10000 iterations. In addition, the error parameters, correlation (R) and Nash-Sutcliffe (NSE) coefficients were investigated for different models with different inputs. The ANFIS model results show more efficiency to predict runoff by increasing the number of inputs as well as increasing the percentage of input data in the training phase (Table 2). This can be achieved by reducing the error parameters, increasing the correlation coefficient, and improving in the NSE coefficient. Also, the model does not provide an acceptable response if only the rainfall data is used to predict runoff, despite the 95% increase in input data even with the minimum or maximum monthly temperature. The performance of the model would not be optimal, in case of entering only the minimum or maximum monthly temperatures, despite the 95% increase in input data. It is because of the negative values of the NSE coefficient. Improving the performance of the model in simulating the precipitation runoff-rainfall process by entering the average temperature to the minimum and maximum monthly temperature is also well visible by the model. The model performance in rainfall-runoff simulation will be improved, if we use the triple values of the average, minimum, and maximum monthly temperature together. Table 2 also shows that the increasing the correlation coefficient, the decreasing the error coefficients. Table 2 reveals that the model performance will be ultimately improved by using all four inputs (i.e., the triple temperature as well as rainfall values) with the correlation and NSE coefficients of 98% and 0.95, respectively (Fig. 3).

Consequently, the volume of runoff during the climate change conditions with respect to the baseline period would be decreased to 0.17 percent. Therefore, this could be a warning for water resources management [17].

Table 2. Analysis of the rainfall-runoff simulation process at Golestan dam reservoir (R_e=0.04 & D_{tr}=95%)

	prediction inputs	$NSE = 1 - \frac{\sum_{i=1}^{n}(Q_O - Q_S)^2}{\sum_{i=1}^{n}(Q_O - \overline{Q_O})}$	$R = \frac{Cov(O,S)}{\delta_O \delta_S}$	$RMSE = \sqrt{\frac{\sum_{i=1}^{n}(e_i)^2}{n}}$	**Number of Fuzzy Rules**
1	Rainfall	**ERROR**	**ERROR**	**ERROR**	**ERROR**
2	Monthly average Minimum temperature	-2.66	0.45	0.09	45
3	Monthly average Maximum temperature	-0.9	0.52	0.09	35
4	Monthly average Minimum temperature Monthly average Maximum temperature Monthly average temperature	0.07	0.27	0.33	175
5	Monthly average Minimum temperature Monthly average Maximum temperature Monthly average temperature	0.27	0.53	0.16	184
6	Monthly average Minimum temperature Monthly average Maximum temperature Rainfall	0.95	0.98	0.02	307

Where Q_o is the observed runoff and Q_s is the simulated runoff.
'N' the total number of runoff data points estimated from the model.
cov is the covariance of δ which is a symbol of standard deviation of simulated values (S) and observed values (O).
e_i is the prediction error - which is obtained from the difference between simulated and observed values.

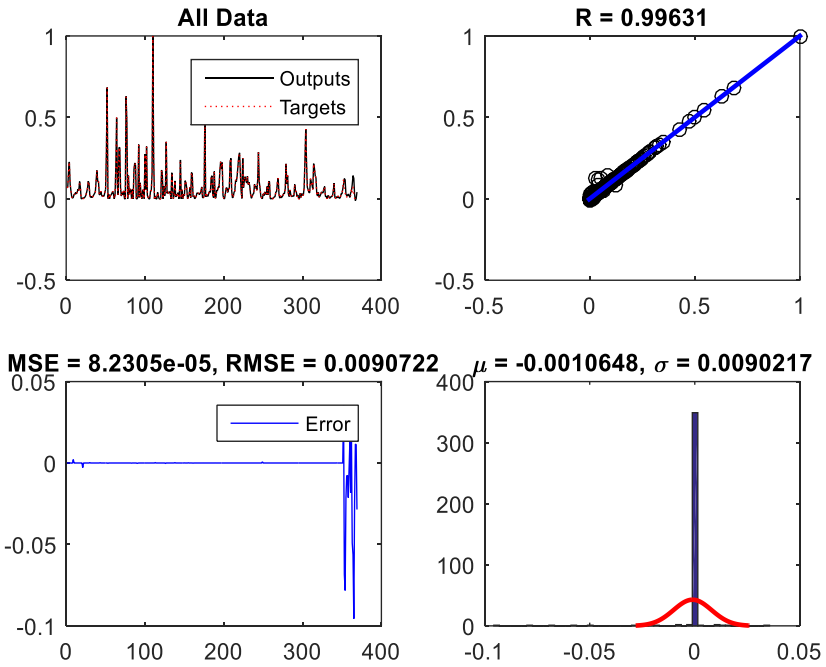


Figure 3. Correlation and error coefficients of the best ANFIS model predictor for Golestan Dam Inflow Runoff (R_e=0.04 & D_{tr}=95%)

4.3. RESERVOIR OPERATION MODEL

The MOFFA algorithm has been used for extracting the operation rules from the Golestan Dam Single-Reservoir System in Golestan province Northeastern Iran (Fig.4), and a downstream network of 4200 hectares. This reservoir has a volume of 43.7 million cubic meters at a normal level, 100 meters above sea level, and 54 million cubic meters at overflow level. The curve of the volume-area of the reservoir was extracted through the following equation with the R2=0.997 correlation coefficient and based on Fig.7:

$$Y = -0{,}002X^2 + 0{,}184X + 1{,}435 \quad (22)$$

The maximum requirements of baseline and climate change are 37.84 and 41.86 million cubic meters. Fig.5 shows the average amount each month of reservoir discharge, the mean depth of evaporation, and the volume of baseline and climate change water demands. The findings indicated that the ratio of discharge into the reservoir and demand for water under climate change circumstances declined by approximately 17 percent and increased by 10 percent, respectively, compared to baseline circumstances.

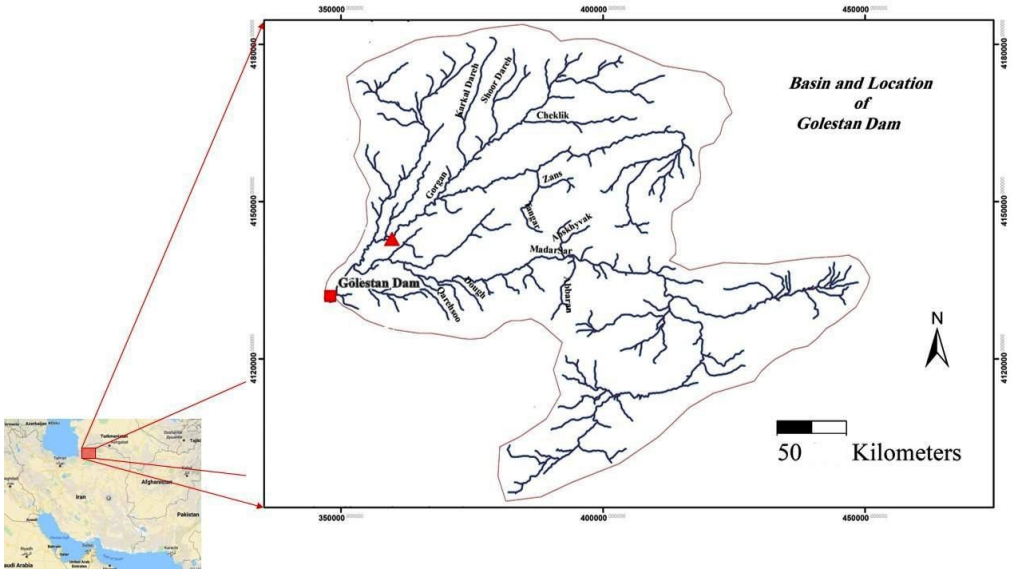


Figure 4. The geographical location of the study region

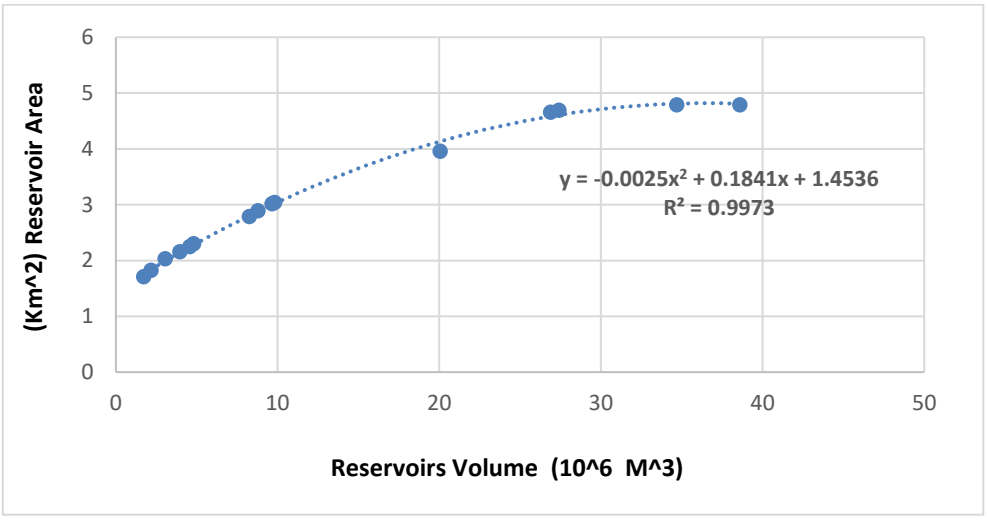


Figure 5. Volume-area curve of Golestan Dam reservoir

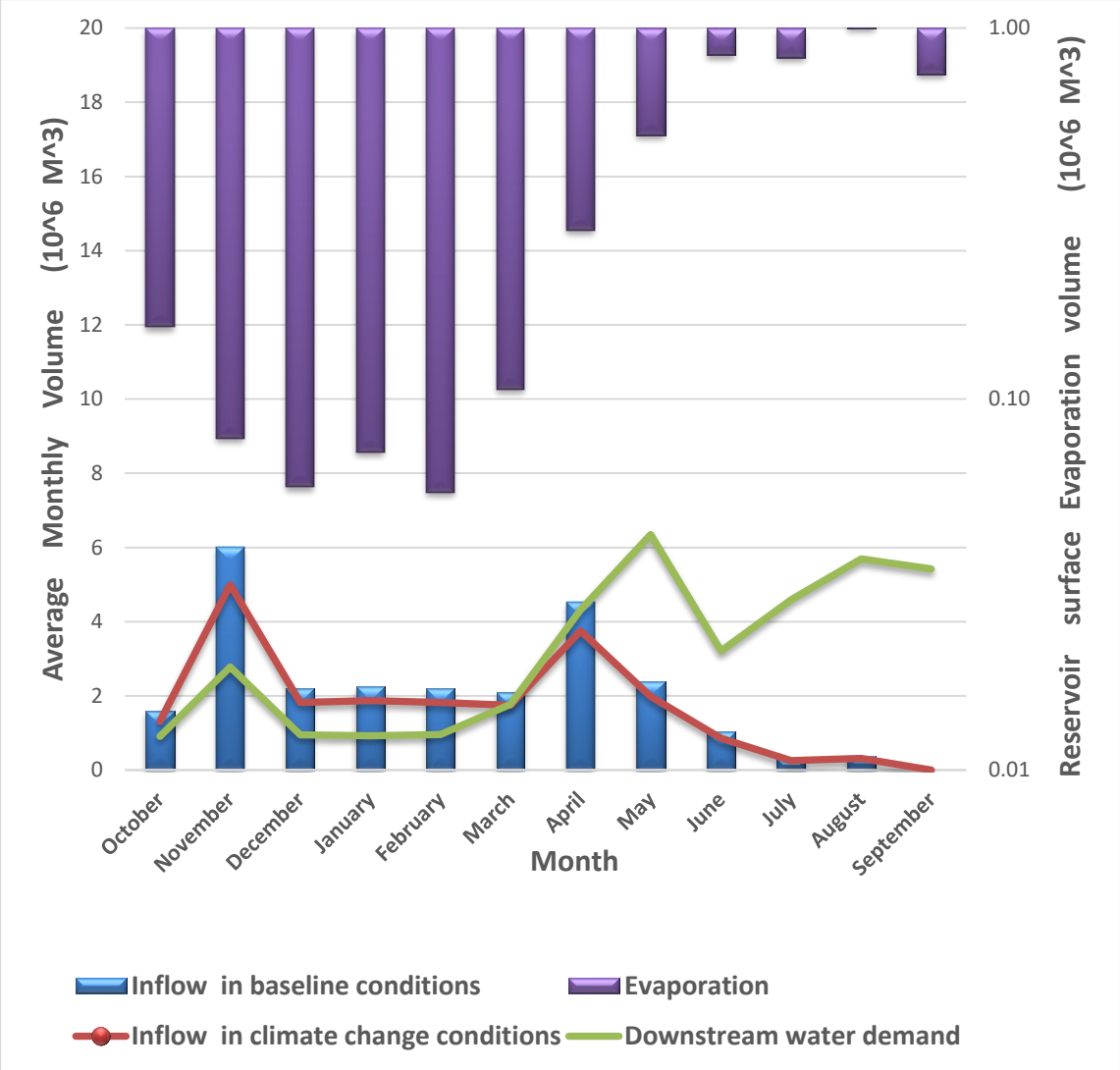


Figure 6. The average monthly release volume, as well as the monthly average evaporation volume and the monthly average demand volume for water under baseline and climate change conditions.

The Golestan Dam reservoir's optimum operation rules were obtained from a two-targeted issue, using the MOFFA algorithm. The two-target issue concerned optimizing the reliability of demand and reducing system vulnerability. (Fig. 6) shows the findings for baseline and climate change circumstances of the two-objective optimization algorithm in the context of the Pareto curve. As reported in (Fig. 7), there are 16% to 45% and 10% to 43% of vulnerability shifts in baseline and climate change circumstances. The number of reliabilities shifts in baseline and climate change circumstances is 47% to 90% and 27% to 93%. Moreover, 29% and 27% of vulnerabilities are created, respectively, for baseline conditions and climate change circumstances for each 75% of reliability. In common words, the extent of climate change vulnerability and reliability is greater than those in the baseline. Each point in the Pareto curve (Fig. 7) demonstrates a reservoir operation rule, including its vulnerability and reliability indices. Neither one of those Pareto points have taken priority over another; they may vary depending on

catchment conditions and policies. The next step was to assess the optimal level of water demand rules in baseline and climate change circumstances. To this end, the optimum rules have been compared with the optimum rules resulting from circumstances of climate change. The findings for the supply of water requirements for the 75 percent reliability index are reported in (Fig. 8a) for the baseline and (Fig. 8b) for the climate change circumstances. The following is assessed for the two options, as stated earlier, compared with the subsequent demand for water by the changes in the volume of shortage by the optimum operation rules resulting from the proposed optimization algorithm. The findings are shown in (Fig. 8b) and (Fig. 9b), respectively.

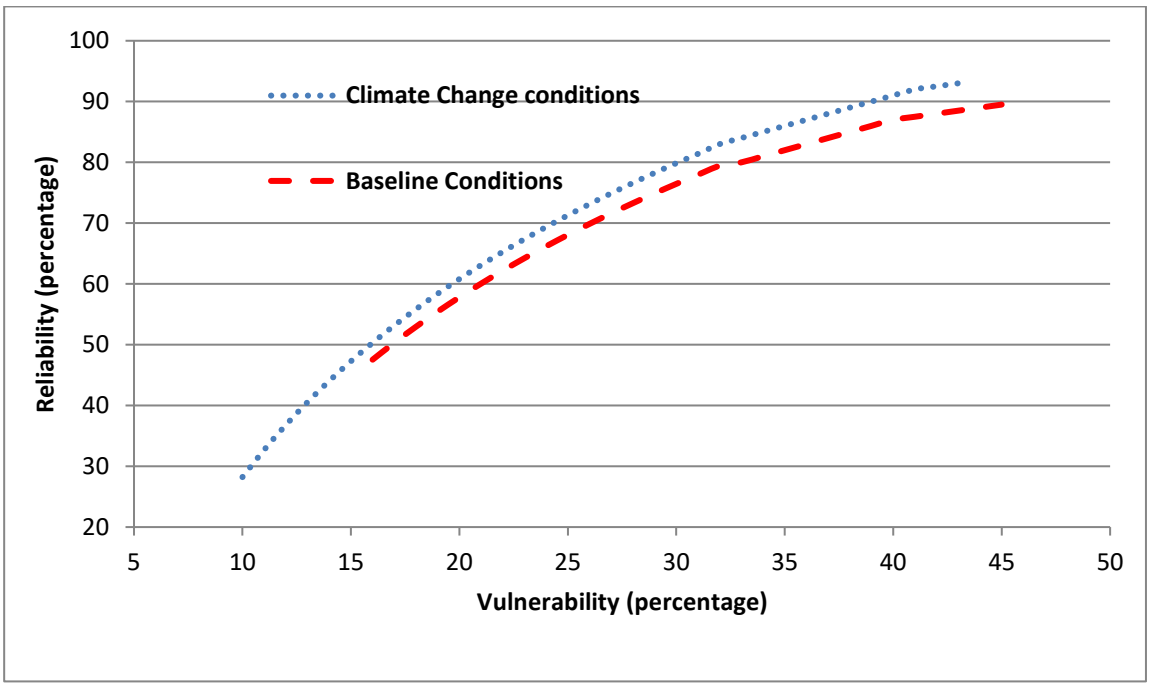
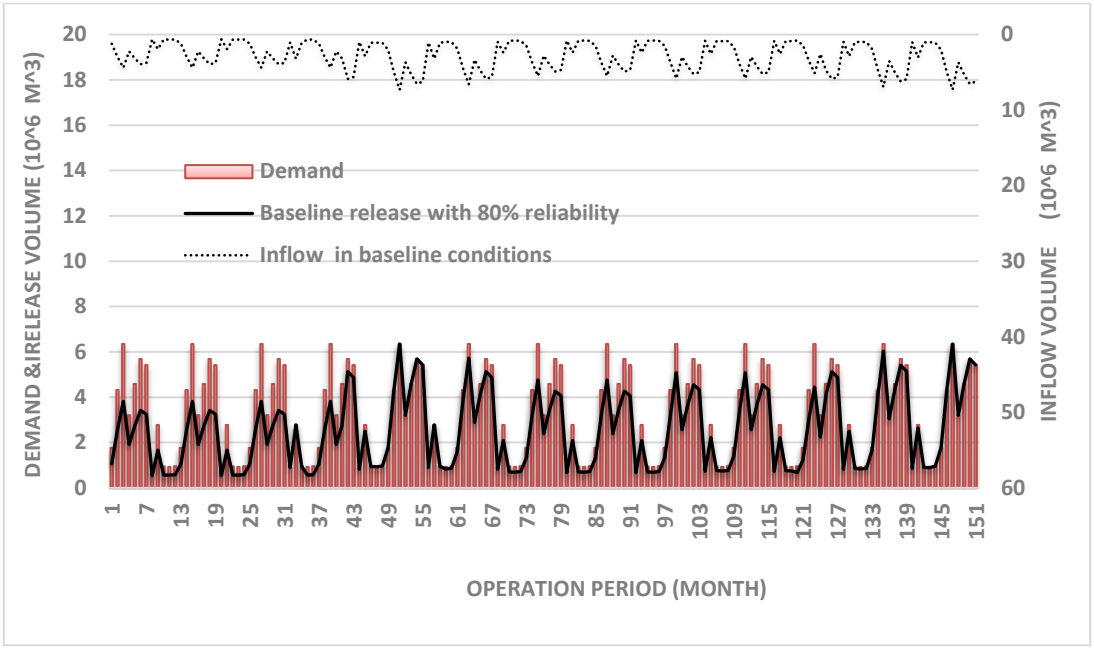
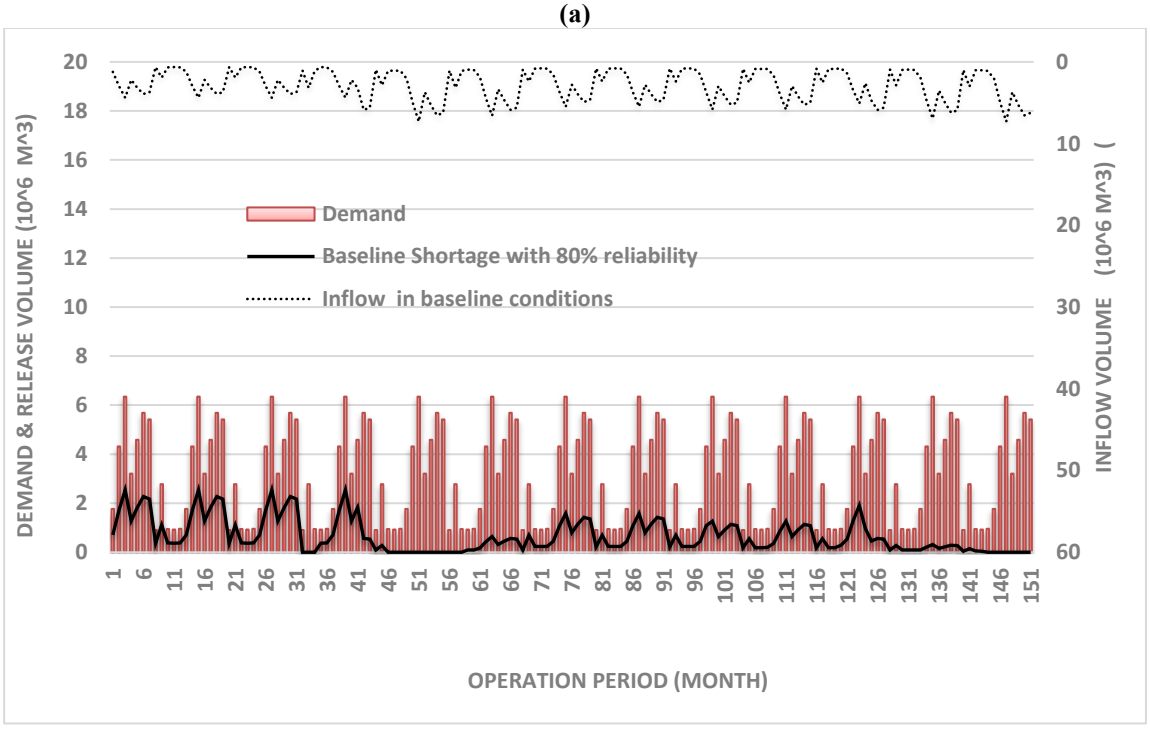


Figure 7. The comparison of the Pareto curve and changes in vulnerability and reliability objective functions.

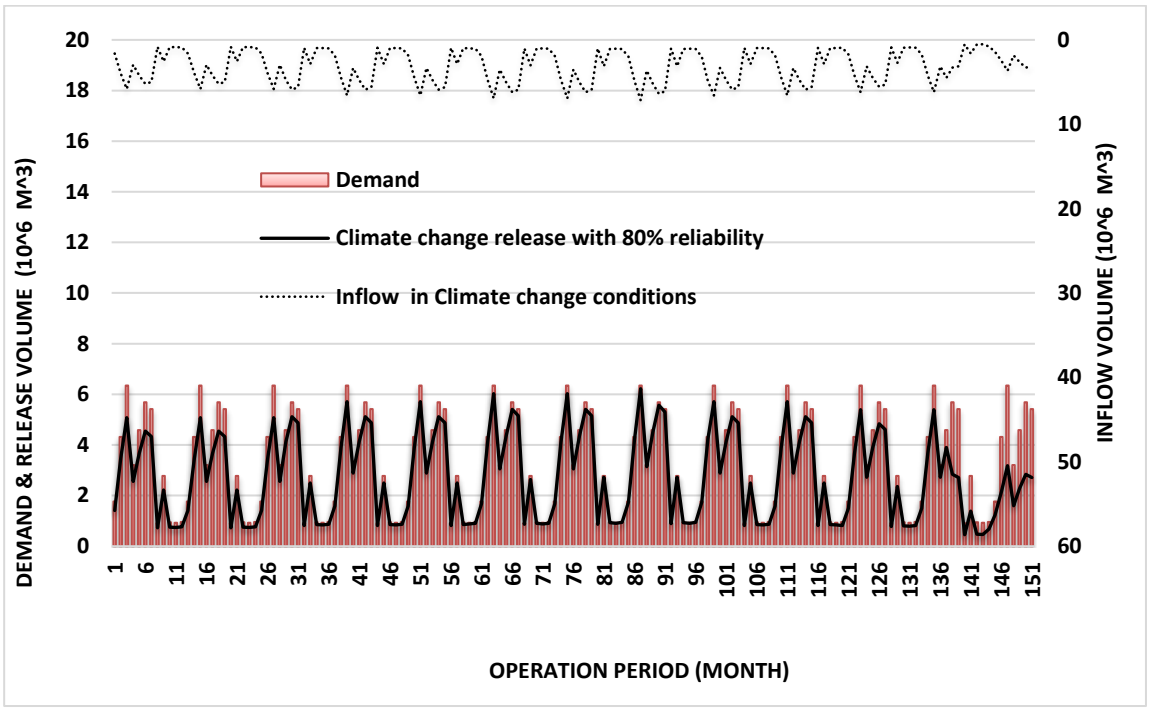


(a)

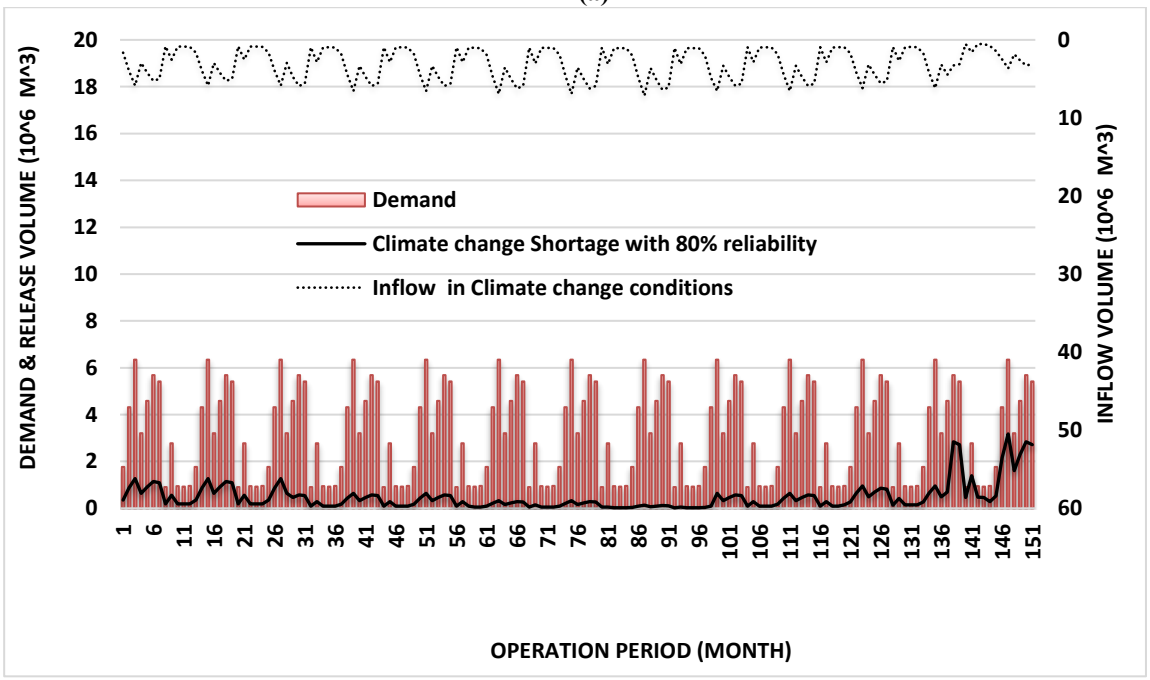


(b)

Figure 8. The comparison of (a) release volume, (b) and shortage volume per each Pareto point resulted from 75% reliability in baseline conditions



(a)



(b)

Figure 9. The comparison of (a) release volume and (b) shortage volume per each Pareto point resulted from 75% reliability in climate change conditions

According to (Fig. 8a) and (Fig. 9a), climate change release rates are greater than under baseline circumstances, which would be 10 percent due to improved demand for water under climate change circumstances. On the other side, (Fig. 8b) and (Fig. 9b) shows that the performance of the dam also increased under the circumstances of climate change. Over the next stage, for evaluating the reservoir performance in providing downstream water requirements, the objective function values of 75 percent reliability per Pareto point have been determined in the circumstances, as stated in (Table 3). According to (Table 3), reservoir release is more consistent with climate change circumstances. The performance of the dam is also stronger under the circumstances of climate change.

Table 3. The comparison of objective functions in baseline and climate change conditions for each Pareto point (75% reliability)

Conditions	Reliability (%)	Vulnerability (%)
Baseline	75	29
Climate Change	75	27

5. Conclusion

One of the most important factors that can be regarded in catchments is to consider all objectives within policies governing the operation of the water resources systems to provide water demand. Thus, it is essential to provide a collection of decision-making options (Pareto Curve) under climate change conditions, so that executive managers could even determine the relative importance of the objectives in this respect. Since every point in the Pareto curve indicates a reservoir operation rule that can be changed under the catchment policies, the extraction of multi-objective reservoir operating rules is inevitable. In the present investigation, the Farmland Fertility Optimization algorithm was first used in water resource engineering management to solve the problem of Golestan Dam's reservoir system in baseline and climate change circumstances in the Golestan province. Objective functions, including maximizing the reliability and minimizing the vulnerability index, were focused on parameters such as the inflow volume to the reservoir, the storage volume and the volume of water demand extracted from the MOFFA algorithm, in order to obtain the reservoir release rules (based on the Pareto curve). The research revealed that the range of vulnerability changes for baseline and climate change circumstances were 16% to 45%, 10% to 43%, and that reliability improvements in baseline and climate change had varied from 47% to 90% and 27% to 93%, respectively. Considering 75% of the reliability index, the vulnerability values were obtained 29% and 27% based on the baseline and climate change circumstances, respectively. Comparing baseline with optimum climate change rules showed that the water demands in the reservoir's release rate would be more in accordance with requirements under climate change circumstances. Therefore, the Golestan Dam reservoir could perform stronger under climate-change circumstances. Afterward, in order to determine the efficiency of the reservoir to satisfy the downstream water demands, the values of the objective function were compared for 75 percent reliability in the above circumstances. The findings revealed that the reservoir release rate is much more in accordance with climate change demand, such that evidence is provided that Golestan Dam performs better under climate change circumstances.

References

1. Akbari H, (2012). Case study of reservoir application using genetic programming, Master Thesis, Faculty of Agricultural Engineering and Technology, University of Tehran.
2. Yeganeh, B. Shafie Pour Motlagh, M. Rashidi, Y. & Kamalan, H. (2012). Prediction of CO concentrations based on a hybrid Partial Least Square and Support Vector Machine model. Atmospheric Environment, 55: 357-365. doi.org/10.1016/j.atmosenv.2012.02.092.
3. Donyaii, A. R., Sarraf, A. P., &Ahmadi, H. (2020a). Optimization of Reservoir Dam Operation Using Gray Wolf, Crow Search and Whale Algorithms Based on the Solution of the Nonlinear Programming Model Journal of Water and Soil Science, In Press. [in Persian].
4. Zamanirad, M., Sarraf, A., Sedghi, H. Saremi, A. & Rezaee, P. (2020). Modeling the Influence of Groundwater Exploitation on Land Subsidence Susceptibility Using Machine Learning Algorithms. Nat Resour Res 29, 1127–1141 https://doi.org/10.1007/s11053-019-09490-9.
5. Ashrafi, S. M. (2019). Investigating Pareto Front Extreme Policies Using Semi-Distributed Simulation Model for Great Karun River Basin. Journal of Hydraulic Structures, 5(1), 75-88.
6. Ashrafi, S. M., Ashrafi, S. F., & Moazami, S. (2017). Developing self-adaptive melody search algorithm for optimal operation of multi-reservoir systems. Journal of Hydraulic Structures, 3(1), 35-48.
7. Wu X, Wei X, and Guo W, 2012. The multi-objective ecological operation model of cascade hydropower reservoirs, 2012. International Workshop on Information and Electronics Engineering (IWIEE), Procedia Engineering, 29:3996 – 4001.
8. Sayyafzadeh, M., Haghighi, M., Bolouri, K., &Arjomand, E. (2012). Reservoir characterization using artificial bee colony optimization. The APPEA Journal, 52(1), 115-128.
9. Hossain, M. S., & El-Shafie, A. (2014). Evolutionary techniques versus swarm intelligences: application in reservoir release optimization. Neural Computing and Applications, 24(7-8), 1583-1594.
10. Ashofteh P S, Bozorg Haddad O, Akbari-Alashti H and Mariño M A, (2014). Determination of irrigation allocation policy under climate change by genetic programming, Journal of Hydrologic Engineering, DOI: 10.1061/(ASCE)IR.1943-4774.0000807, 04014059.
11. Ehteram, M., Karami, H., Mousavi, S. F., Farzin, S., Celeste, A. B., &Shafie, A. E. (2018). Reservoir operation by a new evolutionary algorithm: Kidney algorithm. Water resources management, 32(14), 4681-4706.
12. Donyaii, A. R., Sarraf, A. P., & Ahmadi, H. (2020b). Multi-Objective Optimal Utilization Policy of Boostan Dam Reservoir Using Whale and NSGA-II Algorithms Based on Game Theory and Shannon Entropy Method, Iranian water researches Journal, In Press. [in Persian].
13. Afkhamifar S. & Sarraf, A. P. (2020). Prediction of groundwater level in Urmia Plain aquifer using hybrid model of wavelet Transform-Extreme Learning Machine based on quantum particle swarm optimization. Watershed Engineering and Management, 12(2): 351-364. doi: 10.22092/ijwmse.2019.126515.1669, [in Persian].

14. Nouri M, (2015). Management of multi-objective and multi-reservoir water resources systems using optimization models in climate change circumstances, Ph.D. thesis, Faculty of Civil Engineering, Ferdowsi University of Mashhad.
15. Ashofteh P S andBozorg Haddad O, (2015). Using GP optimization tools developed for the multi-objective operation of reservoirs in climate change, Iranian Journal of Soil and Water Research, Vol. 46, No. 3, pp. 415-422.
16. Shayanfar, H., & Gharehchopogh, F. S. (2018). Farmland fertility: A new metaheuristic algorithm for solving continuous optimization problems. Applied Soft Computing, 71, 728-746.
17. Moazami Goudarzi, F., Sarraf, A. P., & Ahmadi, H. (2020). Prediction of runoff within Maharlu basin for future 60 years using RCP scenarios, Arabian Journal of Geosciences, Vol. 13, No. 14, pp. 1-17.



© 2020 by the authors. Licensee SCU, Ahvaz, Iran. This article is an open access article distributed under the terms and conditions of the Creative Commons Attribution 4.0 International (CC BY 4.0 license) (http://creativecommons.org/licenses/by/4.0/).

